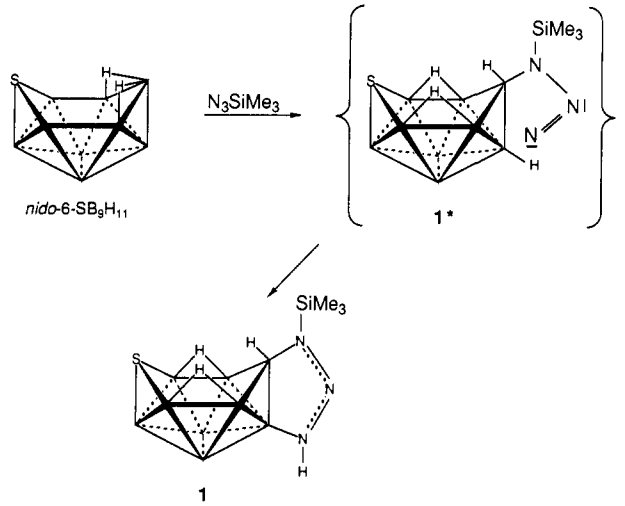

Figure 2. Proposed reaction sequence leading to the formation of (μ_2-(4,*exo*-9)-1-$SiMe_3$-3-H-N_3)-*arachno*-6-SB_9H_{10} **1** from *nido*-6-SB_9H_{11}.

consistent with those observed for other 10-vertex, 26-skeletal-electron systems such as *exo*-9-Et_3N-*arachno*-6-SB_9H_{11},[11] thus indicating that the triazene group is functioning as a two-skeletal-electron donor to the cage. The triazene bridges the B4 and B9 atoms, forming a planar exopolyhedral five-membered ring composed of the three azide nitrogens and the two cage boron atoms. The B4–N3 distance, 1.486 (10) Å, is slightly shorter than the B9–N1 distance, 1.515 (10) Å. Both distances are significantly shorter than the N–B9 distance observed[11b] in *exo*-9-Et_3N-*arachno*-6-SB_9H_{11} (1.600 (4) Å) and fall between the ranges normally observed for boron–nitrogen single (1.57–1.60 Å) and double (1.30–1.43 Å) bonds.[2] The distances and angles for the triazene unit (N1–N2, 1.292 (8) Å; N2–N3, 1.283 (7) Å; N1–N2–N3, 110.7°) are similar to those observed in 1,3-diphenyltriazene (1.32 Å, 1.27 Å, 115°).[12] Surprisingly, the B4–B9 distance (1.698 (10) Å) is only slightly shorter than in *exo*-9-Et_3N-*arachno*-6-SB_9H_{11}, suggesting that the electron delocalization evident in the triazene nitrogen–nitrogen and boron–nitrogen distances does not extend to the cage borons. The remaining intracage distances and angles are similar to those in *exo*-9-Et_3N-*arachno*-6-SB_9H_{11}.[11b]

Because of its strong Lewis acid properties, *nido*-6-SB_9H_{11} is unique among the larger polyhedral boranes. For example, the compound readily forms adducts[11] at the B9 boron with many bases, such as in *exo*-9-Et_3N-*arachno*-6-SB_9H_{11}, and hydroborates olefins and acetylenes by a process that is proposed to involve an initial electrophilic attack on the unsaturated organic by the thiaborane.[13] The formation of **1**, therefore, most likely arises via the reaction sequence outlined in Figure 2. The trimethylsilyl azide is strongly polarized, with the α-nitrogen having a partial negative and the γ-nitrogen a partial positive charge. Therefore, an initial electrophilic attack of the thiaborane would be directed at the α-nitrogen to yield the indicated base-adduct intermediate (**1***) in which the azide is bonded to the exo position of the B9 boron, as in *exo*-9-Et_3N-*arachno*-6-SB_9H_{11}. Subsequent insertion (hydroboration) of the γ-nitrogen of the azide into the B4–H bond would then result in ring closure, yielding the structure observed for **1**.

Preliminary studies of the reactions of benzyl azide with *nido*-6-SB_9H_{11} also indicate the formation of the benzyl analogue of **1**. In addition, the data obtained for minor products produced in both the trimethylsilyl azide and benzyl azide reactions are consistent with the formation of new azathiaborane clusters. The observed stability of **1** suggests that it is not the precursor to these insertion products, and that they may have resulted via an intermediate analogous to **1***, in which the azide is bound to the *endo*-B9 position. We are presently exploring the characterization of these products and the expansion of these azide reactions to the generation of new classes of aza-cage/ring complexes.

Acknowledgment. We thank the Department of Energy, Division of Chemical Sciences, Office of Basic Energy Sciences, and the Deutsche Forschungsgemeinschaft, DFG, for the support of this research.

Supplementary Material Available: Tables of positional parameters, anisotropic temperature factors, bond distances, bond angles, and least-squares planes for **1** (12 pages); listing of observed and calculated structure factors for **1** (10 pages). Ordering information is given on any current masthead page.

(10) Single crystals of **1** were grown at 50 °C over several days in a glass tube in vacuo. Structural data: space group $P2_1/c$, a = 11.027 (1) Å, b = 11.431 (2) Å, c = 12.819 (3) Å, β = 105.12 (1)°, V = 1559.9 (9) Å^3, Z = 4, and d_{calcd} = 1.080 g/cm^3. The structure was solved by direct methods (MULTAN 11/82). Refinement was by full-matrix least-squares techniques based on F to minimize the quantity $\sum w(|F_o| - |F_c|)^2$ with $w = 1/\sigma^2(F)$. Non-hydrogen atoms were refined anisotropically. Positions of cage hydrogens were refined (thermal parameters were fixed at 6.0 Å^2); all other hydrogen atoms were included as a constant contribution to the structure factors and were not refined. Refinement converged to R_1 = 0.076 and R_2 = 0.080.

(11) (a) Hertler, W. R.; Klanberg, F.; Muetterties, E. L. *Inorg. Chem.* **1967**, *6*, 1696–1706. (b) Hilty, T. K.; Rudolph, R. W. *Inorg. Chem.* **1979**, *18*, 1106–1107.

(12) Kondrashev, Y. D.; Gladkova, V. F. *Kristallografiya* **1972**, *17*, 33–40; *Chem. Abstr.* **1972**, *76*, 132697m.

(13) (a) Meneghelli, B. J.; Rudolph, R. W. *J. Am. Chem. Soc.* **1978**, *100*, 4626–4627. (b) Meneghelli, J. B.; Bower, M.; Canter, N.; Rudolph, R. W. *J. Am. Chem. Soc.* **1980**, *102*, 4355–4360.

Singlet–Triplet Separations Measured by Phosphorus-31 Nuclear Magnetic Resonance Spectroscopy. Applications to the Molybdenum–Molybdenum Quadruple Bond and to Edge-Sharing Bioctahedral Complexes

F. Albert Cotton,* Judith L. Eglin, Bo Hong, and Chris A. James

Department of Chemistry and Laboratory for Molecular Structure and Bonding, Texas A&M University College Station, Texas 77843

Received January 13, 1992

Generally speaking, the separation in energy of a low-lying triplet state from a diamagnetic ground state has been estimated (often with great accuracy, as for copper(II) acetate) by measurements of the magnetic susceptibility of the solid compound over a broad temperature range (typically 5–300 K).[1-3] We report here an alternative way to obtain such data that is more convenient, sensitive, and widely applicable for samples in the solid state and solution.[4] We also report results for two important classes of compounds (shown in Figure 1) and important conclusions to be drawn therefrom, such as the δ-electron contribution to the barrier to rotation about the Mo–Mo quadruple bond.

The ^{31}P solution-state NMR spectra of compounds of the types $M_2Cl_4(L\text{-}L)_2$ and $M_2Cl_6(L\text{-}L)_2$, where L-L is a bidentate phosphine ligand, are characterized by variations in the chemical shifts of the phosphorus atoms with temperature. On the basis of a negligible dipolar contribution, the temperature dependence of the ^{31}P chemical shift can be used to calculate the hyperfine coupling constant (A), the diamagnetic chemical shift (δ_{dia}) for

(1) Bleany, B.; Bowers, K. D. *Proc. R. Soc. London* **1952**, *A214*, 451.

(2) Cotton, F. A.; Daniels, L. M.; Dunbar, K. R.; Falvello, L. R.; O'Connor, C. J.; Price, A. C. *Inorg. Chem.* **1991**, *30*, 2509 and references cited therein.

(3) (a) Hopkins, M. D.; Zietlow, T. C.; Miskowski, V. M.; Gray, H. B. *J. Am. Chem. Soc.* **1985**, *107*, 510. (b) Collman, J. P.; Woo, L. K. *Proc. Natl. Acad. Sci. U.S.A.* **1984**, *81*, 2592.

(4) (a) Campbell, G. C.; Haw, J. F. *Inorg. Chem.* **1988**, *27*, 3706 and references cited therein. (b) Boershma, A. D.; Phillippi, M. A.; Goff, H. M. *J. Magn. Res.* **1984**, *57*, 197. (c) LaMar, G. N.; Horrocks, D.; Holm, R. *NMR of Paramagnetic Molecules*; Academic Press: New York, 1973; pp 583.

0002-7863/92/1514-4915$03.00/0

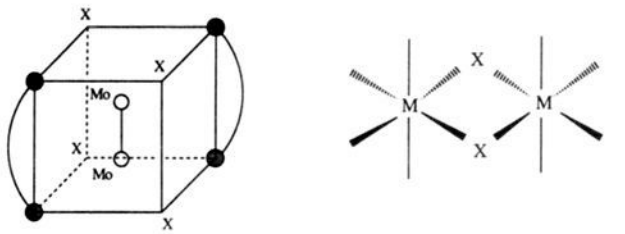

I II

Figure 1. Schematics of $Mo_2Cl_4(L\text{-}L)_2$ (type I) and $Mo_2Cl_6(L\text{-}L)_2$ (type II) complexes.

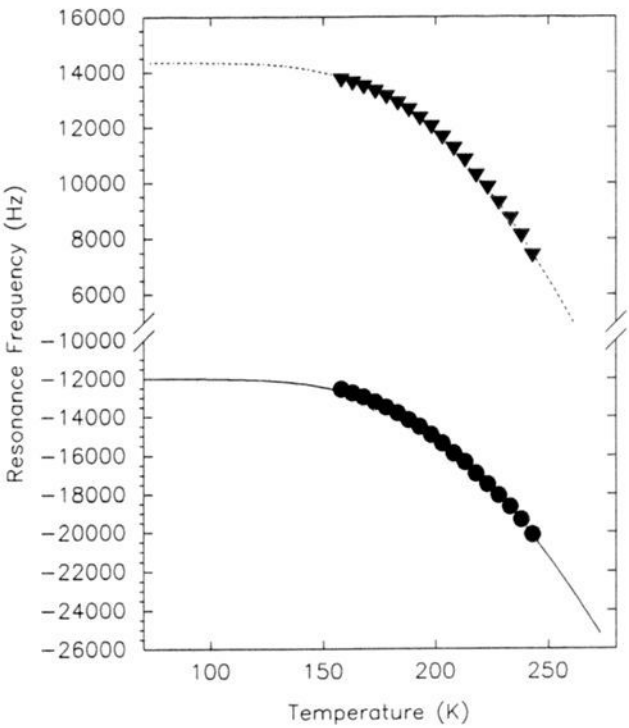

Figure 2. Representation of a typical set of data obtained for $MoWCl_6(dppe)_2$ showing the temperature-dependent chemical shift of the phosphorus atoms bonded to the tungsten atom (solid triangles) and the molybdenum atom (solid circles) as well as the lines fitted to this data with eq 1.

the phosphorus atom, and the singlet state–triplet state energy level splittings ($-2J$) from

$$H_{obsd} = H_{dia} + \frac{2g\beta H_0 A}{(\gamma_P/2\pi)kT}(3 + e^{2J/kT})^{-1} \qquad (1)$$

where H_{obsd} is the frequency of the ^{31}P resonance of the complex being measured, H_{dia} is the frequency the same nucleus would have in a diamagnetic environment, T is the absolute temperature, and the other terms have their usual meanings.[4] This technique requires approximately 5–25 mg of sample, and no ad hoc correction for paramagnetic impurities is necessary. Figure 2 is a graphic representation of a typical set of data collected and the fitted curve.

The first application of this method that we discuss is to the classic problem of how a δ bond in an $X_4M\text{–}MX_4$ type molecule changes as a function of the angle (χ) of internal rotation. Well-known theory[5-9] has shown that, with two atomic δ orbitals to interact and two electrons, four states arise, which should have

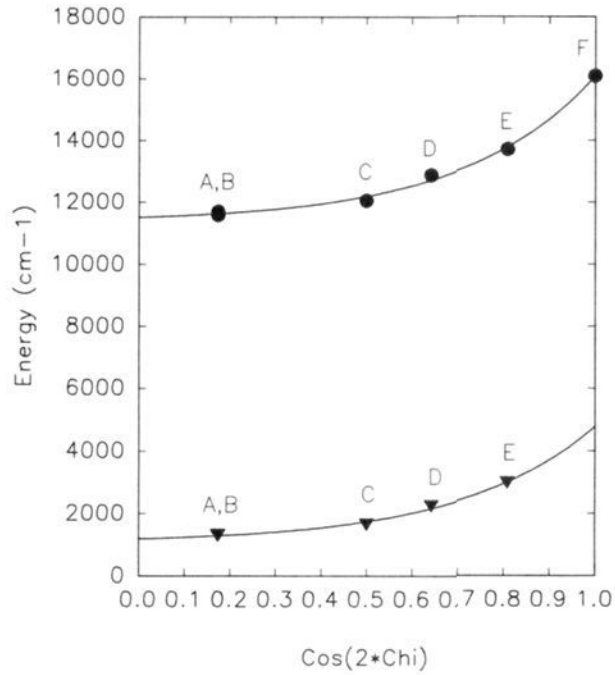

Figure 3. Plot of the $^1(\delta^2)$–$^1(\delta\delta^*)$ (solid circles) and $^1(\delta^2)$–$^3(\delta\delta^*)$ (solid triangles) energy transition versus cos 2χ for a series of $Mo_2Cl_4(L\text{-}L)_2$ complexes.[11]

Table I. Summary of Magnetic Data for $M_2Cl_6(L\text{-}L)_2$ Compounds[a]

phosphine ligand	Mo	W	Mo–W
dppm	1459 (1200)[b]	1231	1451
dppe	1085 (941)[c]	842 (1115)[c]	936

[a] All values are in cm^{-1}. Values in parentheses were obtained from solid-state magnetic susceptibility data. [b] Reference 2. [c] Reference 14.

the energy ordering $^1A_{1g}(\delta^2)$, $^3A_{2u}(\delta\delta^*)$, $^1A_{2u}(\delta\delta^*)$, and $^1A_{1g}(\delta^{*2})$, where the state symbols pertain to an eclipsed (D_{4h}) structure. As χ increases from 0° to 45°, the overlap of the d_δ orbitals goes (linearly with cos 2χ) to 0, and the separation of the δ^2 ground state from the $^3(\delta\delta^*)$ state should decrease. It was shown several years ago[10] that, in a series of molecules of type I, χ varied from 0° to ca. 40° and that the $^1(\delta^2)$–$^1(\delta\delta^*)$ separation decreases so as to asymptotically approach a limiting value (ca. 11 000 cm^{-1}). We have now established the behavior of the $^1(\delta^2)$–$^3(\delta\delta^*)$ separation for a similar set of compounds. Figure 3 shows the results for a series of $Mo_2Cl_4(L\text{-}L)_2$ complexes.[11]

Among the key points established by these results are the following: (1) The two separations maintain an essentially constant difference, indicating that (as expected) the exchange integral K is essentially constant (at ca. 10 000 cm^{-1}). (2) The persistence of configuration interaction, including and in addition to that between the $^1(\delta^2)$ and $^1(\delta^{*2})$ states, assures that the ground state remains $^1(\delta^2)$ even at $\chi = 45$ (where $^3(\delta\delta^*)$ lies 1230 cm^{-1} higher). (3) The δ-electronic contribution to the barrier to rotation about the Mo–Mo quadruple bond was experimentally established to be 9.9 kcal mol^{-1}, with an approximate uncertainty of 0.5 kcal mol^{-1}.[12]

(5) Hansen, A. E.; Ballhausen, C. J. *Trans. Faraday Soc.* **1965**, *61*, 631.
(6) Ballhausen, C. J.; Gray, H. B. *Molecular Orbital Theory*; W. A. Benjamin: Reading, MA, 1964; pp 14–15.
(7) Cotton, F. A.; Walton, R. A. *Multiple Bonds Between Metal Atoms*; John Wiley & Sons: New York, 1983; pp 390–393.
(8) Hopkins, M. D.; Gray, H. B.; Miskowski, V. M. *Polyhedron* **1987**, *6*, 705.
(9) Smith, D. C.; Goddard, W. A. *J. Am. Chem. Soc.* **1987**, *109*, 5580.
(10) Cotton, F. A.; Dunbar, K. R.; Matusz, M. *Inorg. Chem.* **1986**, *25*, 3641.
(11) The band for the $^1(\delta^2) \rightarrow {}^1(\delta\delta^*)$ transition for each complex was recorded in the same solvent as the ^{31}P NMR spectra and the energy of the $0 \rightarrow 0$ vibronic component estimated (see ref 7, Chapter 8). A: $Mo_2Cl_4(dmpe)_2$. B: $Mo_2Cl_4(depe)_2$. C: $Mo_2Cl_4(dppe)_2$. D: $Mo_2Cl_4(dppee)_2$. E: $Mo_2Cl_4(dppp)_2$. F: $Mo_2Cl_4(PMe_3)_4$. (The abbreviations of the bidentate phosphine ligands have their usual meanings.)
(12) A previous attempt[3a] to estimate the δ-electronic barrier in a somewhat similar manner gave 15 kcal mol^{-1}. This result is flawed both by nonquantitative curve fitting and by the unjustified assumption that the energy of the ground state at $\chi = 45°$ would be that of the $^3(\delta\delta^*)$ state. We have taken the extrapolated $^1(\delta^2)$–$^3(\delta\delta^*)$ energies at $\chi = 0°$ (4700 cm^{-1}) and 45° (1230 cm^{-1}) and used the difference (3470 cm^{-1}) to obtain 9.9 kcal mol^{-1}.

The second class of compounds to which we have applied the ^{31}P NMR method are the edge-sharing bioctahedral complexes of molybdenum(III) and tungsten(III) of structure type II. In this case, the M-M interactions consist of fully formed σ and π bonds plus a weak antibonding interaction between δ orbitals.[13] Table I gives values of the energy transition from $^1A_{1g}$ to $^3B_{1u}$ for edge-sharing bioctahedral complexes with metal cores of Mo_2, W_2, and Mo-W and the bidentate phosphines dppm (bridging) and dppe (chelating).

The values of the singlet-triplet separations for edge-sharing bioctahedral complexes obtained using the ^{31}P NMR technique are in reasonable agreement with values previously obtained by solid-state magnetic susceptibility measurements on bulk samples requiring corrections for paramagnetic impurities. In addition to the data presented here for $Mo_2Cl_4(L\text{-}L)_2$ and edge-sharing bioctahedral complexes, studies of other quadruply bonded transition metal complexes as well as additional edge-sharing complexes are in progress.

Acknowledgment. We thank Professor James F. Haw for guiding us to ref 4 and the National Science Foundation for support.

(13) Cotton, F. A. *Polyhedron* **1987**, *6*, 667.
(14) Agaskar, P. A.; Cotton, F. A.; Dunbar, K. R.; Falvello, L. F.; O'Connor, C. J. *Inorg. Chem.* **1987**, *26*, 4051.

Quantized Adhesion Detected with the Atomic Force Microscope

Jan H. Hoh, Jason P. Cleveland, Craig B. Prater, Jean-Paul Revel,† and Paul K. Hansma*

Department of Physics, University of California Santa Barbara, California 93106
Division of Biology, California Institute of Technology, Pasadena, California 91125

Received February 13, 1992

The atomic force microscope (AFM)[1] is rapidly becoming a powerful tool for investigating surface chemistry and adhesion.[2-7] Current efforts with this new instrument are guided by the pioneering research of Israelachvili and his colleagues, whose work with the surface force apparatus has laid the foundation for investigating interactions near and between surfaces.[8-13] The AFM is capable of measuring forces of less than 10^{-11} N with high spatial resolution, thus making possible the study of very weak interactions and local surface chemistry. Here we report the first (to our knowledge) observation of discrete adhesive interactions with measured forces of 1×10^{-11} N. Two mechanisms for this effect are proposed: individual hydrogen bonds between the tip and surface are resolved or ordered water layers create different force minima near the surface.

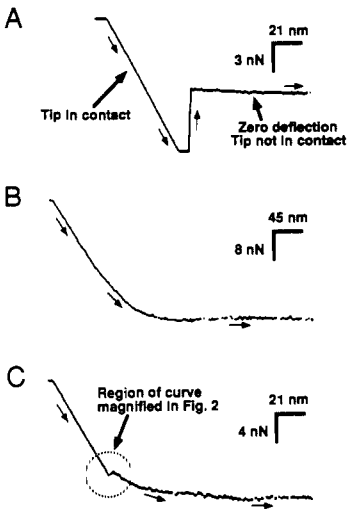

Figure 1. Cantilever deflection versus sample position curves (often called force curves) of a silicon nitride tip breaking contact with a glass surface in water, acquired with digital control. The full scan range is shown. A: At pH 5 a large adhesive interaction of 9×10^{-9} N is evident (the bottom of the trace, with the jump-off point, is off the scale). B: At pH > 9 the interaction became strongly repulsive. C: At pH's between 8 and 9, a small adhesive interaction is present. High-resolution measurements with analog electronics were made when this interaction was near 1×10^{-9} N. The region circled is that examined closely in Figure 2.

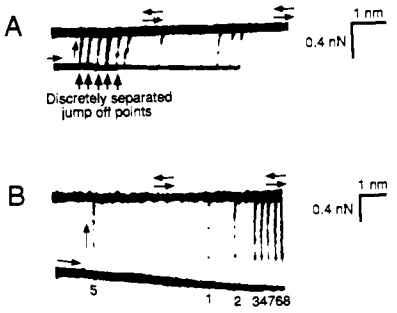

Figure 2. Multiple oscilloscope traces showing discrete jump-off forces of the silicon nitride tip from glass surface at pH 8.5-9. Note that, as in Figure 1, the x axis does not represent the separation distance between tip and sample as is the case for many force versus distance plots; instead, the x axis is the movement of the glass surface mounted to the piezo and the y axis reflects the position of the tip. While the tip is in contact with the surface, the movement of the tip and glass are coupled. This allows us to resolve differences in cantilever deflection *at jump-offs* of less than 10^{-10} m (about 10^{-12} N). A: Traces are from about 12 sequential scans. The left-to-right traces clearly show the discrete cantilever deflections at jump-off. Several events retraced the exact same lines. The top horizontal line is broader because it also contains the approaching trace (right-to-left). The z piezo cycled a total of 180 nm at 0.5 Hz. B: An identical experiment to A in which the relative order of jump-off events was recorded (numbered 1-8). The adhesion increases and decreases randomly, demonstrating that directional drift is not a factor.

We have examined the interaction between a standard silicon nitride microfabricated AFM stylus[14] and a glass surface[15] in water. A NanoScope II scanning probe microscope (Digital Instruments, Santa Barbara, CA) equipped with an AFM stage, D type scanner, and fluid cell was operated in the force mode.[6,7] For the high-resolution measurements, control and output from the AFM stage was switched to an analog wave generator for z input voltage and a storage oscilloscope for the output. The pH of the water (>10 MΩ) was adjusted with NaOH. Fluid in the cell was changed every 10-20 min to compensate for what ap-

† California Institute of Technology.

(1) Binning, G.; Quate, C. F.; Gerber, C. *Phys. Rev. Lett.* **1986**, *56*, 930-933.
(2) Burnham, N. A.; Colton, R. J. *J. Vac. Sci. Technol.* **1989**, *A7*, 2096-2913.
(3) Landman, U.; Luedtke, W. D.; Burnham, N. A.; Colton, R. J. *Science* **1990**, *248*, 454-461.
(4) Ducker, W. A.; Senden, T. J.; Pashley, R. M. *Nature* **1991**, *353*, 239-241.
(5) Butt, H. J. *Biophys. J.* **1991**, *60*, 777-785.
(6) Weisenhorn, A. L.; Hansma, P. K.; Albrecht, T. R.; Quate, C. F. *Appl. Phys. Lett.* **1989**, *54*, 2651-2653.
(7) Weisenhorn, A. L.; Maivald, P.; Butt, H.-J.; Hansma, P. K. *Phys. Rev. Lett. B*, in press.
(8) Israelachvili, J. N. *Proc. Natl. Acad. Sci. U.S.A.* **1987**, *84*, 4722-4724.
(9) Israelachvili, J. N. *Intermolecular and Surface Forces*, 2nd ed.; Academic Press: New York, 1992.
(10) Israelachvili, J. N.; Pashley, R. M. *Nature* **1983**, *306*, 249-250.
(11) Israelachvili, J. N.; McGuiggan, P. M. *Science* **1988**, *241*, 795-800.
(12) Israelachvili, J. N. *Acc. Chem. Res.* **1987**, *20*, 415-421.
(13) Israelachvili, J. N.; Pashley, R. *Nature* **1982**, *300*, 341-342.
(14) Albrecht, T. R.; Akamine, S.; Carver, T. E.; Quate, C. F. *J. Vac. Sci. Technol. A* **1990**, *8*, 3386-3396.
(15) This is a glass cover slip used as a sample substrate in many of our imaging experiments: Hoh, J. H.; Lal, R.; John, S. A.; Revel, J. P.; Arnsdorf, M. F. *Science* **1991**, *253*, 1405-1408. It is manufactured from standard soda lime glass.

0002-7863/92/1514-4917$03.00/0